Improved image analysis using digital media technology

YangBo Li[1]*, ZeYu Xu[2], Dong Sun[1]

[1]*Department of Computer Science and Technology, Henan Mechanical and Electrical Engineering College, Xinxiang Henan, China*

[2]*Material Science and Engineering, Zhengzhou University, Zhengzhou, Henan, China*

Abstract

Digital image correlation and image registration or matching are among the most widely used techniques in the fields of experimental mechanics and computer vision, respectively. Despite their applications in separate fields, both techniques primarily involve detecting the same physical points in two or more images. In recent years, with the requirement of high-resolution and real-time measurement, the computation speed of digital image correlation (DIC) has become increasingly important. At present, the DIC algorithms based on the iterative spatial domain cross-correlation algorithm are widely recognized as the most robust and rapid. In this paper, the integral image technique is extended to handle the complex items in the equations of the DIC algorithm in order to accelerate the calculation process. The influence of the interpolation method on the performance of the DIC algorithm is also investigated. In addition, the analysis of computational complexity and numerical experiment results are presented to illustrate the effectiveness of this method. The results successfully verify that the proposed method can improve the computation speed of the DIC algorithm greatly, and the improvement is more notable when the fast interpolation method is utilized. In this paper a modification of a high-speed correlation system for the purposes of mechanical structures modal parameters estimation is described. Together with hardware modification an original version of a program Modan 3D was created, which is a complex tool for execution of an experimental and operational modal analysis.

Keywords: improved image analysis, digital media technology, digital image correlation

1 Introduction

Digital image correlation (DIC) and image registration or matching (hereinafter referred to as "IRM ") are currently among the most widely used techniques in the fields of experimental mechanics and computer vision, respectively [1]. Their popularity and prevalence originate from the rapid evolution of computer and imaging technology. The DIC technique has been used in the mechanics and optics fields for deformation, shape and motion measurements, whereas the IRM technique has become an essential process in computer vision for numerous applications in a variety of fields. Despite that the DIC and IRM techniques are being used in different applications, both techniques mainly involve detecting the same physical points in two or multiple images. In this paper, a brief comparison of the two techniques is presented, and their complements are described. The goal is to introduce some valuable achievements in computer vision to experimental mechanics.

The measurement accuracy is the first important concern of any measuring method. Early work s on the accuracy of DIC primarily focused on the study of the error assessment [2-5]. In recent years, the works on the measurement accuracy were mainly conducted to improve the robustness of the DIC. For example, Zhang et al. [6] used a ring template and quadrilateral element to improve the accuracy of the DIC for the large rotation measurement, and Pan et al. [7] proposed the incremental calculation method for a large deformation measurement with the reliability-guided DIC technique. The computation speed is the other important concern in the research of the DIC, and this has become more important in recent years due to the increasing demand for real-time processing and high-resolution measurements. Although different types of methods could be utilized for the DIC computation, such as discrete relaxation labelling methods and modern optimization methods including simulated annealing, evolutionary algorithms, genetic algorithms, particle swarm optimization (PSO), and ant colony optimization (ACO) [8]. The iterative spatial domain cross-correlation algorithms such as the forward additive Newton – Raphson method [10] are the most popular and effective for the DIC calculation due to their robustness and high speed [9]. These algorithms utilize an iterative process to retrieve the displacement fields, which could optimize the correlation function, and every iteration the incremental deformation parameters are obtained to update the parameters of the current estimate. The quality of the initial estimate may affect the convergence property and the convergence speed of the iterative process and thus is critical to the DIC [1, 11, 12]. Pan [7] proposed the reliability-guided DIC, which could improve the quality of the initial estimate by optimizing the computational order of the subsets, and the result verified that the robustness and the computation speed of the reliability-guided DIC is better than that of the general DIC algorithms. The inverse compositional algorithm, which was proposed by Baker [13], is an

---

effective subset matching algorithm because, in this algorithm, the Hessian matrix remains constant and could be computed only once in each subset matching process. Each iteration repeated interpolation should be performed. Therefore, the performance of the interpolation algorithms greatly influences the overall performance of the DIC algorithm. Pan [14] proposed a method to accelerate the interpolation algorithm by caching the inner parameters. The integral image, which is also known as a summed area table, is an effective technique to accelerate the computation of the sum of in a rectangular region [15, 16]. This technique is extraordinarily useful when the sum of values in a rectangular region is queried frequently. The integral image technique is applied widely in the fields of computer graphic and computer vision such as texture mapping [17], face detection [18] and the creation of scale- and rotation-invariant detectors and descriptors [19]. Additionally, Huang et al. [20] applied this technique to find the initial estimate in the DIC computation.

In this paper, an inverse compositional DIC algorithm using the integral image to speed the calculation of Hessian matrix is presented. The accuracy of this algorithm is the same as that of the existing inverse compositional algorithm because their mathematics equation is equivalent. The time complexity of the algorithm is analysed, and the performance of the algorithms is verified by the numerical experiments.

2 Related works

In the past couple of decades, there has been a dramatic increase in the capacity of computer processors making it possible to success-fully simulate complex systems. However, in order to fully validate the models used in these simulations there is the increasing need to get accurate and detailed quantitative experimental data. Over the years, different techniques for probing the dynamics of fluidized bed have been developed. These techniques generally fall into one of two main categories: intrusive or non-intrusive techniques. The intrusive techniques are largely based on resistance, impedance, inductance, piezoelectric or thermal probes while the non-intrusive techniques are mostly based on photographic, X-ray, light scattering or laser techniques [21]. The intrusive techniques, to some extent, however, interfere with the dynamics of beds, unlike the non-intrusive techniques. In recent years, the advances in digital imaging systems and pro-cessing have led to an increase in the application of photography in the study of lab-scale fluidized beds. It is particularly suitable for pseudo-2D gas–solid systems where the inter-phase boundary is easy to detect and the effect of bed depth is minimal. Caicedo et al. [22] used data collected from a CCD camera to deter-mine the influence of reduced velocity on the shape factor and aspect ratio of bubbles formed in a 2Dfluidized bed. Lim et al. [3] investigated the distributions of bubble pierced length as well as some other bubble size measures, experimentally, by employing Digital Image Analysis methods. Hull et al.

[24] developed semi-empirical correlations for the average size and rise velocity of bubbles in a 2D-bubbling fluidized bed, with and without simulated horizontal tube bundles, using digitized images captured with a CCD camera. Goldschmidt et al. [25] developed a whole-field, non-intrusive, Digital Image Analysis technique to study the dynamics and segregation rates in pseudo-2D dense gas-fluidized beds. In their work, a 3-CCD color camera was used to demonstrate that, using binary mixture of particles, the local mixture composition could be determined within 10% accuracy. Furthermore, they showed that even small bubbles and voidage waves could be detected with their technique. However, by working with a camera of limited capacity and by carrying out the image processing directly in the RGB color spectrum, the accuracy of their technique was rather limited. Shen et al. [26], using the image processing toolbox of Matlab achieved a high level of automation in the acquisition, processing and analysis of digitized images of two-dimensional bubbling fluidized beds captured with a digital video camera. They used the time-average data from the images to obtain bubble diameter, velocity, bubble number density and gas through flow. Bokkers et al. [27] substituted the fluid seeds in PIV with bed particles to obtain particle velocity fields in 2D fluidized bed experiments monitored with a monochrome high-speed digital camera. An image analysis technique, based on the computation of the cross correlation of bubble images with multiple spatial resolutions, was proposed by Cheng et al. [28] for measuring the bubble velocity fields at high bubble number density in two dimensional swarms. In their work, the PIV algorithm gave better results, compared to several PTV schemes, because of its robustness in measuring the optical and dynamic characteristics of bubbles. Some works have extended the application of photography to 3D beds. Zhu et al. [29] determined the size distribution of nanoparticle agglomerates at the top of a cylindrical fluidized bed after analysing the images captured with a CCD camera. Also, Wang et al. [30] used laser-based planar imaging, with the aid of a high-resolution digital CCD camera, to determine the shape and size of aggregates in nanoparticle fluidization experiment carried out in a column with rectangular cross-section. In addition to information on the dynamics of bubbles, the dynamics of mixing and segregation is often desired. With the exception of Goldschmidt et al. [25], none of the aforementioned works are able to predict the time evolution of the extents of segregation in poly disperse systems. In this work, the non-intrusive Digital Image Analysis (DIA) technique implemented by Goldschmidt et al. [25] was improved by utilizing a state-of-the-art photographic apparatus and a new image processing procedure to measure in-situ the degrees of segregation in poly disperse systems, particularly in binary and ternary systems, by differentiating colour particles by the unique colour they express in pixels.

3 Digital media based image analysis

The basic of the program Modan 3D consists in an acquisition of the frequency response functions in every virtual grid corner point (labelled as mask point) of the investigated object and their subsequent processing leading to the modal parameters estimation. A broadband object excitation is performed by a modal hammer only in one location – it concerns the method with one input and a multiple output (SIMO).

3.1 THE ACQUISITION OF INPUT DATA

The data acquisition from the modal hammer has been enabled by two special additional apparatuses - CCLD amplifier and AD/DA converter. A block scheme of connection between high-speed correlation system and additional devices, which together serve for realization of experimental modal analysis, is depicted on the Figure 1.
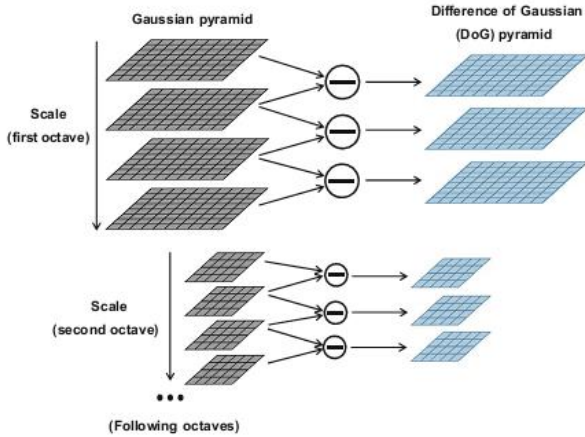

FIGURE 1 Scale-space pyramid for SIFT. The image is subsampled by two in every octave

For such a created system a special script in Matlab has been written, by which it is possible to record an input signal and activate trigger for ensuring the recording of cam-eras image. The algorithm for experimental modal analysis consists of three main parts. While the first one is fully automated, in the second and the third one, respectively, the user intervention is necessary. The outputs of the first part are two modes estimation functions, where in ideal instances the peaks should determine the object natural frequencies. In the second part the user chooses the frequencies that are subjected to analyses by MAC criterion. The last step is the graphical visualization of the mode shapes with corresponding damping ratios for the chosen frequencies. The exported data from the program Istra4D in a form of HDF5 (HDF – Hierarchical Data Format) files are the basic elements for a work with the program Modan 3D. As indicates the format name, it concerns hierarchically structured file. Uppermost are the groups containing subsets, datasets, attributes, or the connections and some information about the data type as well, which describe their character and way of

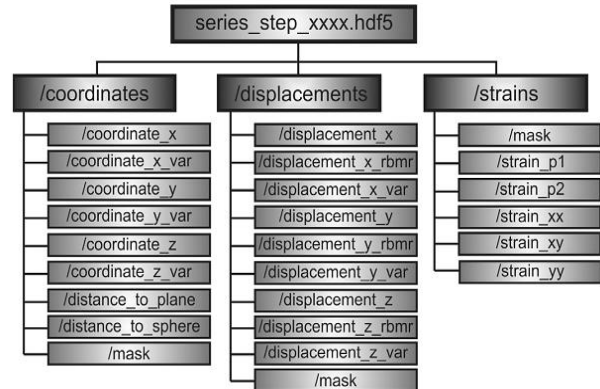interpretation. Istra4D generates the HDF5 file with a structure depicted in Figure 2.

FIGURE 2 HDF5 file exported by the program Istra4D

It contains three main groups (coordinates, displacements and strains), whereby each of them consists of several datasets with the amounts of the quantities measured in mask points. The number of these points is dependent on a size of virtual grid specified in the correlation parameters setup. The points with the value 1 represent the correlated locations. If the value is 0, it concerns either unfilled places or the parts of investigated objects, which from some reason could not be correlated. The total size of mask is then expressed as a product of maximal quantum of mesh rows and columns. The file mentioned above can be simply processed in the program Matlab. This is a main reason, why also Modan 3D is created in this program. In the first step of algorithm the program reads all the measurements data and creates the relevant data matrices needed for next mathematical processing. The mentioned data are time dependence of a force impulse from a modal hammer recorded by AD/DA converter. Three-dimensional data matrices created from HDF5 files containing some information about evaluation mask, spatial coordinates of its points and displacements of these points in directions x, y and z. Taking into account that the calculation of each quantity is performed in all three axes simultaneously. Graphical visualizations of matrices depicted in the next parts are delimited just for the processing of displacements in Z direction.

The program can automatically identify all the maxima of CMIF. On the bases of this, it creates the matrix of frequencies, which it considers as natural ones and by the using of the half-power method [8] it calculates the damping ratios for the each identified natural frequency. Here the first automatic part of the algorithm is ending and for the next processing of the results the user intervention is needful. The user by visual control chooses such frequencies, which he considers as natural ones, after then he de-fines them to the program and it automatically depicts the MAC matrix of corresponding modal vectors. For the visualization of the mode shape the user has to put into the Modan 3D a consecutive number of the frequency from the frequency sequence, for which the mode shape

will be depicted. From the corresponding frequency response matrices the algorithm reads the real parts of all elements and multiplies them by a chosen magnification factor. It adds such obtained values to the reference coordinates of the mask points and creates new matrices of the mask points' coordinates, which are subsequently smoothed by the using of smoothing functions. All reference coordinates of the mask points are thus transformed into a new form corresponding to the object mode shape. The mode shape is finally depicted in color with an associated color scale, which defines the displacements of particular mask points by the unit force application. Such a technique allows investigation of proportionally damped structures.

3.2 BUBBLE DETECTION

The images captured with the digital camera have to be pre-processed before the particle analysis can be conducted. The first step is to identify the relatively large gas voids in the images. This can on one hand aid in evaluating bubble size distribution in the bed and on the other hand remove areas in the images that are likely to pose problems during particle analysis. In the pre-processing, the bubbles, which although contain some particles, can be removed because the amount of particles they contain is negligible. The bubble detection is carried out by a Matlab script written specifically for that purpose. In the script the images are first cropped to remove the bed bottom compartment and side walls. The image is then filtered to remove the background scatter by setting a threshold for the Saturation attribute of the HSV color space. Thereafter, some thresholds are set for both the Hue and Saturation attributes to detect the particles in the images without making distinctions among the particle species. At this step, a fixed, same color is assigned to all the particles identified, hence the image is converted to a gray scale by discarding the Hue and Saturation information while retaining the Value. By setting a threshold for the Value attribute, the voids are made distinct from particle positions. Furthermore, the Sobel edge-emphasizing filter is used to make the edges of the particles more distinct. However, the voids obtainable at this stage do not necessarily constitute a bubble because some voids are just too small to be classified as one, hence the need to more distinctly identify larger pockets of gas voids as bubbles. To achieve this, a very coarse imaging filter is applied to smear the edges of the voids and a threshold is set on the Value attribute to carve out large voids as bubbles. The areas identified as bubbles are then subtracted from the original image by rendering them as black.

3.3 CALIBRATION

When spherical particles of different sizes are randomly packed in a pseudo-2D fluidized bed, the smaller particles tend to appear in a proportion which is more than their

actual composition when the bed is viewed from the side. The smaller particles more readily fit into the void spaces between the larger particles and this effect is even more pronounced when the diameter ratios of the particles are higher. In order to more accurately determine the particle compositions in various areas of the bed, on which several parameters defining bed behavior depend, calibration under actual conditions is crucial. Once again, to demonstrate the calibration technique, the procedure and results for a bid is perse mixture of particles containing various compositions of the 1.5 mm and 2.5 mm species are presented. In the calibration conducted by Goldschmidt et al. [25], a bed with a known composition was first fluidized at a velocity well above that required from incipient fluidization, to thoroughly mix the particles, before the flow was stopped abruptly. The image of the bed is then taken and analysed for the calibration. In this work, in addition to static bed measurements, 'in-situ' calibration using images captured in fluidized states were conducted. This was possible because even at relatively large particle velocities the enhanced capacity of the image capturing apparatus deployed in this work eliminates motion-blur effects.

Furthermore, ordinarily, the calibration profiles would be expected to exhibit a high degree of symmetry about the axis orthogonal to the ideal relation at the middle of the chart but this is not the case. The deviation from the ideal relation is found to be more pronounced when the larger 2.5 mm particles are present at relatively low volumetric fraction in the bed. This behaviour is somewhat analogous to the trend seen in the packing fractions of FCC-ordered binary mixtures where the deviation from the mono disperse packing fraction is more when the larger particle is less in proportion.

A parity plot of the calculated mass percentage of the 2.5 mm particles, evaluated solely from the images captured and the calibration fit, against the mass percentage that was actually present in the bed was prepared as a verification measure. To calculate the mass percentage from the images, the bed was divided into many cells in both the horizontal and vertical directions and the composition in each cell was evaluated with the calibration fit. The average composition in the bed was then computed by taking the average of the composition in all cells while weighing each cell with the amount of particles (pixels) detected in them. However, since the smaller particles more often than not appear more in the grids this region of the fit is not really of paramount importance. More cells fall in the range below 70% composition. The largest error margin obtained in this region was ±1.92% at 40% composition and the average error margin was ±1.64%. In terms of deviation from the ideal relation, a similar trend is observed with the percentage deviation which is slightly higher in the region below 70% composition. Generally, the fit can be said to be very accurate.

3.4 DISCRETE ELEMENT SIMULATIONS

Although series of segregation experiments can be carried out in the lab for different poly disperse systems with a variety of fluidization conditions, it is very hard, if not impossible, to compare the segregation results obtained via the DIA technique with the "exact" conditions inside the bed. One alternative is the use of simulation models like the Discrete Element Method (DEM) model which provides exact information about the size and position of every particle in the bed. The DEM is essentially a Euler–Lagrange model in which the gas phase is treated as a continuum and solved using Navier Stokes equations, whereas the particles are tracked individually by solving the Newtonian equations of motion with a collision model to account for the non-ideal particle. More details about the DEM model used in this work can be found. It is important to note that the robustness of the flow solver and the flow-particle coupling is not very relevant here. The major requirements are some degree of randomness in the particle positions, a variety of segregation scenarios and availability of a realistic visualization tool. In addition, it is desirable that the collision parameters be such that the extent of overlap is reduced to the barest minimum. For verification and validation, the newly developed DIA technique was used to evaluate the time evolution of segregation in the visualizations of some DEM simulations that was conducted prior to this study. The DEM contact time and spring stiffness were adequate in keeping maximum and mean particle overlap below 1 and 0.05% respectively. For a realistic visual representation of the DEM data, an Open Visualisation Tool, The OVITO, was used. The visualization software, by employing a powerful concept of data processing pipeline, produces a meaningful depiction of the particle based simulation data. In the algorithm, ambient lighting calculations and shading of atoms are implemented so that the images produced can as close as possible, mimic camera snapshots of actual fluidized beds. An adequate calibration profile of the binary mixture is essential in the implementation of the DIA technique for the evaluation of segregation profiles. Simulation runs that mimic the steps conducted hitherto, for lab experiments, would require lots of computational time and resource, hence a calibration chart was sought from the available simulation series. The DEM code was adapted to provide directly the number of each particle type with their centers of mass in the Eulerian cells. Since the Eulerian cell size is only 1.32 times the size of the 2.5 mm particle, the grid was enlarged to 3 Eulerian cells in the vertical and horizontal di-rections. Hence, initially, a 10×10 mm grid was used in the DEM image analysis. However, this grid size was found to be too small be-cause of the fuzziness in the pro file it generated in its calibration chart, consequently, the grid size had to be increased even further. A 30×30 mm grid was found to be adequate for generating a calibration chart provides a distinct trend. Hence, it is proposed that the grid size used in the image

analysis should be up to 10 times the largest particle diameter to obtain a meaningful calibration fit.

4 Experimental modal

The experimental modal analysis by the using of high-speed correlation system was realized on two steel specimens with the shapes and dimensions. The thickness of both sheets was 0.8 mm. There was a difference in the specimens restrains – the first one was fixed along its narrower edge and the second one was attached in its center of gravity to a pedestal. Both specimens were excited by a modal hammer with plastic head. The cameras sample frequency has been set to 2000 fps and the total acquisition time was chosen to 1s. Acquired data with the information about displacements of particular mask points was exported in HDF5 format and processed in Modan 3D subsequently. As the measurements were performed in laboratory conditions, where the noise had no influence on investigated objects, it was not necessary to weight the response signal by exponential window. To minimize the influence of leakage several weighting functions were tried out. Finally for the input and output frequency spectra calculation the Kaiser weighting function was used, by which the best results were achieved. For a verification of the reached results reliability a system specialized for vibration analysis was used. The sys-tem manufactured by Brüe l& Kjær consists of the analyser PULSE LAN-XI. The excitation of specimens was performed with the modal hammer Brüel & Kjær 8206 and for the recording of corresponding responses a laser-doppler vib-rometer Polytec PDV100 was used. A schematic visualization of excited and investigated specimens points with marked sampling directions of input and output quantities can be seen in Figure 3.
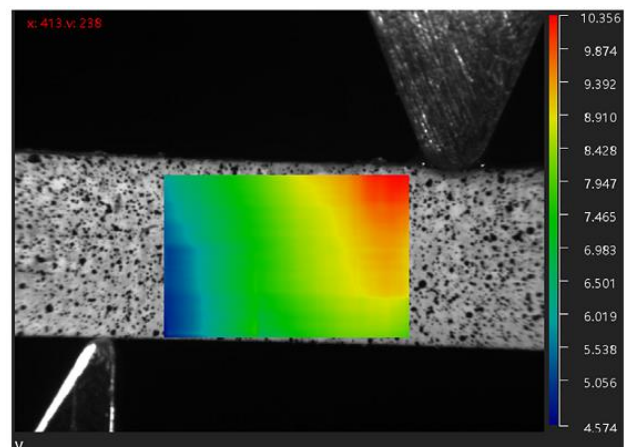

FIGURE 3 The result of the three-point bending test

The first specimen included 64 investigated points and a point labeled as 65 was the location of excitation. The second specimen contained 48 points subject to the analysis of vibration velocity and the 25th point was the location of modal hammer impacts as well. The point corresponding to the center of this specimen was not

analyzed, because in this place the sheet was attached. The realization and processing of the measurement were done in the software PULSE Labshop. The differences in magnitudes are due to the fact that while Modan 3D uses the amplitudes of vibration for frequency response functions calculation, the data obtained by vibrometer are obtained in a form of vibration velocity. Likewise the number of points, in which FRFs were deter-mined, is distinct – by the using of Modan 3D ca. 3600 locations and by vibrometer only 64, respectively 48 locations were evaluated. By the analysis of the acquired graphs it was possible to identify particular modes of investigated specimens. Determined natural frequencies together with corresponding mode shapes and calculated damping ratios of individual modes. The hole in the evaluated schema of the second specimen pictured by the results from Modan 3D, corresponds to a screw female, by which the sample was attached to the pedestal. This part was by the definition of evaluation mask left out.

5 Conclusions

In summary, the integral image technique is used to accelerate the DIC algorithms without sacrificing the measurement accuracy. Based on the theoretical analysis and experimental results, the following conclusions can be obtained:

(1) With the integral image technique, the computation of the item in the form of the sum in a rectangular region can be sped up effectively, and its complexity is reduced from O(nm)to O(1).

(2) The Hessian matrix computation could be accelerated by the integral image technique. The improvement is more significant when the workload of the other part is less.

(3) The integral image technique could be widely applied to many types of DIC algorithms, such as the inverse compositional algorithms using the SSD criterion or ZNSSD criterion.

(4) The interpolation scheme has significant influence on the overall performance of the DIC algorithms as each iteration of the matching process involves many interpolation operations.

References

[1] Sutton MA, Orteu J, Schreier H 2009 Image correlation for shape, motion and deformation measurements: basic concepts, theory and applications *New York: Springer Verlag*

[2] Wang YQ, Sutton MA, Bruck HA, Schreier HW 2009 Quantitative error assessment in pattern matching: effects of intensity pattern noise, interpolation, strain and image contrast on motion measurements. Strain 2009 45(2) 60–78

[3] Bornert M, Brémand F, Doumalin P, Dupré JC, Fazzini M, Grédiac M, et al. 2009 Assessment of digital image correlation measurement errors: methodology and results ExpMech 2009 49(3) 53–70

[4] Lecompte D, Smits A, Bossuyt S, Sol H, Vantomme J, Van Hemelrijck D, et al. 2006 Quality assessment of speckle patterns for digital image correlation *Opt Lasers Eng* **44**(11)32–45

[5] Tao H, Xie H, Wang S 2010 Evaluation of the quality of a speckle pattern in the digital image correlation method by mean subset fluctuation *Opt Laser Technol* **43**(1) 9–13

[6] Zhang X, Chen J, Wang Z, Zhan N, Wang R 2012 Digital image correlation using ring template and quadrilateral element for large rotation measurement *Opt Lasers Eng* **50**(7) 22–8

[7] Pan B, Dafang W, Yong X 2012 Incremental calculation for large deformation measurement using reliability-guided digital image correlation *Opt Lasers Eng* **50**(4) 86–92

[8] Boykov Y, Veksler O, Zabih R 2001 Fast approximate energy minimization via graph cuts *IEEE Trans Pattern Anal Mach Intell* **23**(11) 22–39

[9] Hu Z, Xie H, Lu J, Zhu J 2010 Study of the performance of different subpixel image correlation methods in 3D digital image correlation *Appl Opt* **49**(21) 44–51

[10] Bruck HA, McNeill SR, Sutton MA, Peters WH 1989 Digital image correlation using Newton– Raphson method of partial differential correction *Exp Mech* **29**(3) 61–77

[11] Vendroux G, Knauss WG 1998 Submicron deformation field measurements: Part 2. Improved digital image correlation *Exp Mech* **38**(2) 86–92

[12] Zhao JQ, Zeng P, Lei LP, Ma Y 2012 Initial guess by improved population-based intelligent algorithms for large inter-frame deformation measurement using digital image correlation *Opt Lasers Eng* **50**(3) 73–90

[13] Baker S, Matthews I 2004 Lucas-Kanade 20 years on: a unifying framework *Int J Comput Vis* **56**(3)21–55

[14] Pan B, Li K, Tong W 2013 Fast, robust and accurate digital image correlation calculation without redundant computations *Exp Mech* 1–13

[15] Viola P, Jones M 2001 Robust real-time object detection *Int J Comput Vis*

[16] Lienhart R, Kuranov A, Pisarevsky V 2003 Empirical analysis of detection cascades of boosted classifiers for rapid object detection *Pattern Recognit* 297–304

[17] Crow FC 1984 Summed-area tables for texture mapping *ACM SIGGRAPH Comput Gr ACM* **18**(3) 207–12

[18] Viola P, Jones M 2001 Robust real-time object detection *Int J Comput Vis* **4** 34–47

[19] Bay H, Ess A, Tuytelaars T, et al 2008 Speeded-up robust features (SURF) *Comput Vis Image Underst* **110**(3) 46–59

[20] Huang J, Zhu T, Pan X, Qin L, Peng X, Xiong C, et al 2010 A high-efficiency digital image correlation method based on a fast recursive scheme *Meas Sci Technol* **21**(3) 35-45

[21] McGlone J, Mikhail E, Bethel J 2013 Manual of photogrammetry *Bethesda, Mary-land USA ASPRS*

[22] Peters W, Ranson W 1982 Digital imaging techniques in experimental stress analysis *Opt Eng* **21**(3) 27–31

[23] Sutton M, Wolters W, Peters W, Ranson W, McNeill S 1983 Determination of displacements using an improved digital correlation method *Image Vis Comput* **1**(3) 33–9

[24] Peters W, Ranson W, Sutton M, Chu T, Anderson J 1983 Application of digital correlation methods to rigid body mechanics *Opt Eng* **22**(6) 38–42

[25] Chu T, Ranson W, Sutton M, Peters W 1985 Applications of digital image correlation techniques to experimental mechanics *Exp Mech* **25**(3) 32–44

[26] Sutton M, Cheng M, Peters W, Chao Y, McNeill S 1986 Application of an optimized digital correlation method to planar deformation analysis *Image Vis Comput* **4**(3) 43–50

[27] Bruck H, McNeill S, Sutton M, Peters W 1989 Digital image correlation using Newton–Raphson method of partial differential correction *Exp Mech* **29**(3) 61–75

[28] Pan B, Qian K, Xie H, Asundi A 2009 Two-dimensional digital image correlation for in-plane displacement and strain measurement: a review *Meas Sci Technol*

[29] Sutton M, Orteu J, Schreier H 2006 Image correlation for shape, motion, and deformation measurements *New York, USA: Springer*

[30] Brown L 1992 A survey of image registration techniques *ACM Comput Surv* **24**(4) 25-36

Authors

Yangbo Li, 1982-06, Henan Xinxiang, China.

Current position, grades: lecturer, Henan Mechanical and Electrical Engineering College.
University studies: master's degree in 2009.
Scientific interest: computer application, digital media technology.

Zeyu Xu, 1993-08, Henan Xinxiang, China.

University studies: undergraduate students of Zhengzhou University.
Scientific interest: computer application, material science and engineering

Dong Sun, 1980-01, Henan Xinxiang, China.

Current position, grades: lecturer, Henan Mechanical and Electrical Engineering College.
University studies: master's degree Henan Mechanical and Electrical Engineering College in 2009.
Scientific interest: computer application.